A Flexible and Computationally Efficient Density Model for the Multilook Polarimetric Covariance Matrix

Paul R. Kersten
No affiliation

Stian Normann Anfinsen
Department of Physics and Technology, University of Tromsø, Norway

Abstract

We propose a complex Wishart-Kotz–type I distribution for the polarimetric covariance and coherency matrix. This is a very flexible density model for multilook polarimetric radar data, which can account for severe radar texture with different characteristics. Contrary to alternative models, the closed form expression of the distribution contains no special function, which makes its application to image analysis algorithms both computationally efficient and numerically stable. Parameter estimators based on the method of matrix log-cumulants have been developed and the flexibility of the new distribution has been favourably compared to some common models.

1 Introduction

Polarimetric radar is an important remote sensing instrument which is able to discriminate between different scattering mechanisms and characterise physical properties of the target that cannot be determined from single polarisation radar measurements. This paper is concerned with statistical modelling of the polarimetric sample covariance or sample coherency matrix, that are equivalent data formats representing multilook polarimetric radar data. Parametric models of the probability density function (pdf) for the covariance matrix are important tools in the construction of image analysis algorithms. For instance, the simplest and most common model is the complex Wishart distribution, which has been applied to e.g. speckle filtering [1], classification [2], and change detection [3] of polarimetric synthetic aperture radar (PolSAR) images.

The Wishart model assumes that the speckle in the radar image is fully developed, and it does not consider spatial variation in the mean reflectivity, commonly referred to as radar texture [4]. This is problematic, since the effect of texture become more and more prominent as the resolution of deployed PolSAR sensors continues to improve. Alternative models, such as those based on the multilook polarimetric product model [1], decompose the covariance matrix into a product of two random variates: a positive scalar term accounting for texture and a complex Wishart distributed matrix representing speckle. This approach has lead to accurate models that have been verified on real data, such as the matrix-variate K distribution [5], G^0 distribution [6], and U distribution [7]. The respective models have been successfully incorporated in algorithms for unsupervised classification [8], supervised classification [9], and segmentation [10], to mention some applications.

A drawback of the product model distributions is that they contain mathematical special functions, such as the Bessel K function and the Kummer U function. These functions have a high computational cost and the numerical evaluation of each relies on multiple approximations in order to cover different parts of the domains of the function parameters and independent variables. Lack of smoothness between the approximations as well as failure to cover the entire domains cause problems and instabilities that make it challenging to implement them in software. We here promote the complex Wishart-Kotz–type I distribution (hereafter referred to as the $WK(I)$ distribution) as a candidate model which overcomes these difficulties.

The proposed $WK(I)$ distribution is a generalisation of the complex Wishart distribution, introduced in the real case by Díaz-García and Gutiérrez-Jáimez [11]. It is based on the assumption that the scattering vector has a complex Kotz-type distribution [12]. The $WK(I)$ distribution we present here is not the most general form, which extends the Wishart distribution with three new parameters. The given version is restricted to two additional shape parameters, that still add considerable flexibility and allow both heavier tails and different shapes of the distribution body.

Section 2 introduces the data format of multilook polarimetric radar data and two density models for such data: the traditional complex Wishart distribution and the proposed $WK(I)$ distribution. Section 3 derives the Mellin kind statistics, including matrix log-cumulants that define efficient parameter estimators for the $WK(I)$ distribution. In Section 4 we demonstrate the ability of the proposed density to model texture, as compared to other competitors, by visualisation of the model in a log-cumulant diagram. Conclusions are given in Section 5.

2 Data Models

The measurements of a fully polarimetric radar can be expressed in terms of the scattering vector

$$\mathbf{s} = [S_{xx}\ S_{xy}\ S_{yx}\ S_{yy}]^T , \quad (1)$$

where $(\cdot)^T$ denotes the transposition operator. The vector dimension d is the number of polarimetric channels, and the vector elements are complex-valued scattering coefficients, dimensionless numbers that describe the transformation of incident to backscattered electromagnetic field for all combinations of the two orthogonal transmit and receive polarisations, denoted by subscripts x and y.

While $\mathbf{s}$ is known as the single-look complex data format, this paper is only concerned with multilook complex data. Multilooking is an averaging process which reduces the data amount and suppresses the noise-like effect of multipath backscatter interference, known as speckle, at the expense of reduced spatial resolution. Thus, polarimetric radar data are represented in the intensity domain by the complex sample covariance matrix

$$\mathbf{C} = \frac{1}{L}\sum_{\ell=1}^{L} \mathbf{s}_\ell \mathbf{s}_\ell^H \quad (2)$$

or a linearly transformed version of $\mathbf{C}$, the sample coherency matrix [4]. Here, L is the equivalent number of looks averaged in the process [13] and $(\cdot)^H$ is the Hermitian (conjugate transposition) operator. The random matrix $\mathbf{C} \in \Omega_+ \subset \mathbb{C}^{d\times d}$ is defined on the cone Ω_+ of positive definite complex Hermitian matrices.

If we assume that the distribution of $L\mathbf{C}$ is the true complex Wishart distribution, then $\mathbf{C}$ follows the scaled complex Wishart distribution [14], given by

$$p_{\mathbf{C}}(\mathbf{C}; L, \boldsymbol{\Sigma}) = \frac{L^{Ld}}{\Gamma_d(L)} \frac{|\mathbf{C}|^{L-d}}{|\boldsymbol{\Sigma}|^L} \operatorname{etr}(-L\boldsymbol{\Sigma}^{-1}\mathbf{C}) \quad (3)$$

where $|\cdot|$ is the determinant, $\operatorname{etr}(\cdot) = \exp(\operatorname{tr}(\cdot))$ with $\operatorname{tr}(\cdot)$ as the trace operator, $\Gamma_d(L)$ is the multivariate gamma function of the complex kind [14], $\boldsymbol{\Sigma} = \mathrm{E}\{\mathbf{C}\}$ is the scale matrix, and $L \geq d$ assures that $\mathbf{C}$ is nonsingular. This is denoted $\mathbf{C} \sim s\mathcal{W}_d^{\mathbb{C}}$ and referred to in the remainder of the paper as the Wishart distribution.

If $L\mathbf{C}$ follows the complex equivalent of the real distribution given in [11, Th.3.1], the pdf of $\mathbf{C}$ becomes

$$p_{\mathbf{C}}(\mathbf{C}; L, \boldsymbol{\Sigma}, \rho, \beta) = c\, \frac{|\mathbf{C}|^{L-d}}{|\boldsymbol{\Sigma}|^L} \operatorname{tr}(\boldsymbol{\Sigma}^{-1}\mathbf{C})^{\beta-1} \exp\big(-[L \operatorname{tr}(\boldsymbol{\Sigma}^{-1}\mathbf{C})]^\rho\big) \quad (4)$$

with the constant normalisation factor

$$c = \frac{\rho\, L^{\beta+Ld-1}}{\Gamma\left(\frac{\beta+Ld-1}{\rho}\right)} \frac{\Gamma(Ld)}{\Gamma_d(L)} , \quad (5)$$

where $\Gamma(\cdot)$ is the standard gamma function, $\rho > 0$ and $\beta > 1 - Ld$ are shape parameters, and $\boldsymbol{\Sigma}$ is still the scale matrix parameter, but we note that $\boldsymbol{\Sigma} \neq \mathrm{E}\{\mathbf{C}\}$. Instead, we have

$$\mathrm{E}\{\mathbf{C}\} = \frac{\Gamma\left(\frac{\beta+Ld}{\rho}\right)}{\Gamma\left(\frac{\beta+Ld-1}{\rho}\right)} \frac{\boldsymbol{\Sigma}}{Ld} . \quad (6)$$

Eq. (4) is what we shall refer to as the $W\!K(I)$ distribution. No derivations are given in this paper due to the limited space, neither for the $W\!K(I)$ pdf nor other expressions presented in Section 3. Derivations will be included in a future journal paper.

To visualise the effect of the shape parameters, we have plotted the univariate version of (4) for various values of ρ and β in Figure 1. This pdf will be referred to as the gamma-Kotz–type I distribution, denoted by $\Gamma K(I)$, and is given as

$$p_I(I; L, \sigma, \rho, \beta) = \frac{L^{\beta+L-1}}{\Gamma\left(\frac{\beta+L-1}{\rho}\right)} \frac{\rho}{\sigma} \left(\frac{I}{\sigma}\right)^{\beta+L-2} \exp\left(-\left[\frac{LI}{\sigma}\right]^\rho\right) . \quad (7)$$

In the figure, the mean of all pdfs has been normalised to unity using (6).

Note that the parameter values $\rho = \beta = 1$ reduce (4) and (7) to the Wishart distribution and the gamma distribution, respectively. When $\beta = 1$, (7) can be recognised as the generalised gamma ($G\Gamma$) distribution, proposed as a model for radar images in [15] and [16]. Accordingly, (4) with $\beta = 1$ is named the generalised Wishart–type I distribution, denoted $GW(I)$, while (4) with $\rho = 1$ is termed the generalised Wishart–type II distribution, written as $GW(II)$. The difference between the models will be highlighted in the log-cumulant diagrams of Section 4.

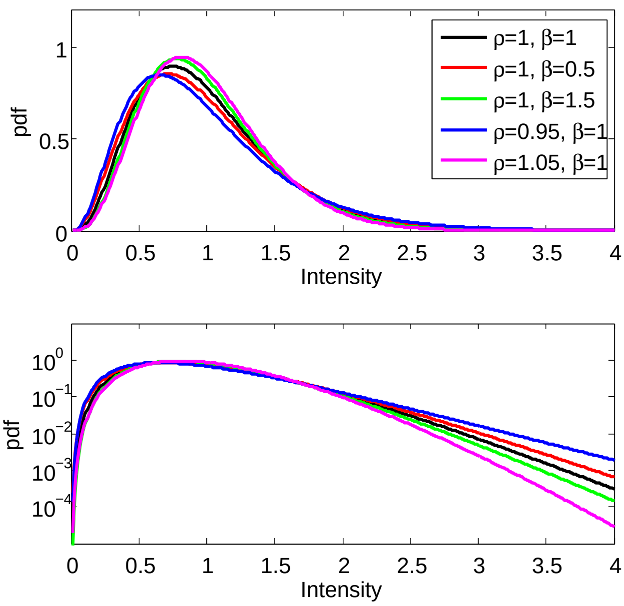

Figure 1: Example of $\Gamma K(I)$ distribution pdfs for different values of the shape parameters ρ and β on linear (top) and semilogarithmic (bottom) scale.

3 Mellin Kind Statistics

Mellin kind statistics were introduced in [17] and extended to the polarimetric case in [14, 18] as an efficient tool for the statistical analysis of multilook radar data. It is based on the Mellin transorm, which is used to analyse the radar images on logarithmic scale.
The Mellin kind characteristic function (ch.f.) of $\mathbf{C}$ is defined as [18]

$$\phi_{\mathbf{C}}(s) = \mathcal{M}\{p_{\mathbf{C}}(\mathbf{C})\}(s) = \mathrm{E}\{|\mathbf{C}|^{s-d}\}\,, \tag{8}$$

where $\mathcal{M}\{\cdot\}(s)$ is the matrix-variate Mellin transform [18] and $s \in \mathbb{C}$ is the complex transform variable. For the $W\!K(I)$ distribution, it evaluates to

$$\phi_{\mathbf{C}}(s) = \phi_{\mathbf{W}}(s) \times \frac{\Gamma(dL)}{\Gamma(d(L+s-d))} \frac{\Gamma\left(\frac{\beta+d(L+s-d)-1}{\rho}\right)}{\Gamma\left(\frac{\beta+dL-1}{\rho}\right)} \tag{9}$$

where we have identified the term

$$\phi_{\mathbf{W}}(s) = \frac{|\mathbf{\Sigma}|^{s-d}}{L^{d(s-d)}} \frac{\Gamma_d(L+s-d)}{\Gamma_d(L)} \tag{10}$$

as the Mellin kind ch.f. of the random matrix $\mathbf{W} \sim s\mathcal{W}_d^{\mathbb{C}}$ from [18]. Thus, (9) can be factorised into a speckle contribution, $\phi_{\mathbf{W}}(s)$, and a pure texture contribution obtained as $\phi_{\mathbf{C}}(s)/\phi_{\mathbf{W}}(s)$. It follows that $\mathbf{C}$ can be decomposed by the well-known product model as $\mathbf{C} = \mathcal{T}\mathbf{W}$, where $\mathcal{T}$ is a scalar positive random texture variable, even though the pdf of $\mathcal{T}$ has not been identified.
Matrix log-cumulants (MLCs) are scalar statistics found as polynomials in the matrix log-moments defined as $\mu_\nu\{\mathbf{C}\} = \mathrm{E}\{(\ln|\mathbf{C}|)^\nu\}$, where ν is the order. The first three moment-to-cumulant relations are

$$\kappa_1\{\mathbf{C}\} = \mu_1\{\mathbf{C}\}\,, \tag{11}$$

$$\kappa_2\{\mathbf{C}\} = \mu_2\{\mathbf{C}\} - \mu_1\{\mathbf{C}\}^2\,, \tag{12}$$

$$\kappa_3\{\mathbf{C}\} = \mu_3\{\mathbf{C}\} - 3\mu_1\{\mathbf{C}\}\mu_2\{\mathbf{C}\} + 2\mu_1\{\mathbf{C}\}^3\,. \tag{13}$$

By definition, the νth-order MLC of $\mathbf{C}$ can be retrieved from the Mellin kind ch.f. through [18]

$$\kappa_\nu\{\mathbf{C}\} = \frac{d}{ds} \ln \phi_{\mathbf{C}}(s) \bigg|_{s=d}\,. \tag{14}$$

The MLCs have proven to be very powerful when applied in method-of-moments type estimation algorithms for the parameters of PolSAR data distributions. They have also provided improved visualisation of the fit of PolSAR data density models to real data, and in particular with respect to texture content [18].
By the additive property of cumulants under the product model [18], we have

$$\kappa_\nu\{\mathbf{C}\} = \kappa_\nu\{\mathbf{W}\} + d^\nu \kappa_\nu\{\mathcal{T}\}\,, \tag{15}$$

where $\kappa_\nu\{\mathcal{T}\}$ is the univariate νth-order texture log-cumulant (TLC) of $\mathcal{T}$. The TLCs isolate the texture contribution. They can be computed from (15) after inserting the MLCs of fully developed speckle, known as [18]

$$\kappa_\nu\{\mathbf{W}\} = \begin{cases} \psi_d^{(0)}(L) + \ln|\mathbf{\Sigma}| - d\ln L & : \nu = 1\,, \\ \psi_d^{(\nu-1)}(L) & : \nu > 1\,, \end{cases} \tag{16}$$

where $\psi_d(\cdot)$ is the multivariate polygamma function [18]. The TLCs under the $W\!K(I)$ distribution have been derived from (4), (14) and (15) as

$$\kappa_\nu\{\mathcal{T}\} = \frac{1}{\rho^\nu}\psi^{(\nu-1)}\left(\frac{\beta+dL-1}{\rho}\right) - \psi^{(\nu-1)}(dL)\,. \tag{17}$$

Estimation of the shape parameters in a Kotz-type distribution in nontrivial, even though progress was made in [19]. We propose to use a method-of-moments type algorithm which solves simultaneaously for ρ and β by numerical inversion of the second and third-order MLC equations. Similar methods have been used with success to estimate the shape parameters of the K, G^0 and U distributions [18], and results for the $W\!K(I)$ distribution will be shown in a journal paper.

4 Model Comparison

A TLC diagram is a plot of $\kappa_3\{\mathcal{T}\}$ versus $\kappa_2\{\mathcal{T}\}$, which can display simultaneously the attainable population moments of given models and sample moments computed from data. In this paper we confine ourselves to plotting the former. The population TLCs $\kappa_2\{\mathcal{T}\}$ and $\kappa_3\{\mathcal{T}\}$ measure the logarithmic scale relative variance and skewness of a covariance matrix distribution with respect to the Wishart distribution. They effectively characterise the amount and type of texture, respectively.
By showing that

$$\lim_{\beta\to 1-Ld} \frac{\kappa_3\{\mathcal{T}\}}{\kappa_2\{\mathcal{T}\}} = -\infty\,, \quad \lim_{\rho\beta\to 0,\, \beta\to\infty} \frac{\kappa_3\{\mathcal{T}\}}{\kappa_2\{\mathcal{T}\}} = 0 \tag{18}$$

it can be proven that $W\!K(I)$ distribution spans the entire upper left quadrant of the TLC diagram. This is shown in Figure 2. It is seen that the $GW(I)$ distribution (magenta curve) closely resembles the K distribution (red curve), whereas the $GW(II)$ distribution (green curve) has a much lighter tail. It is heavier than the Wishart distribution (black circle) though, as seen from the excess logarithmic variance. Nevertheless, the truly interesting model is the $W\!K(I)$ distribution (yellow surface), since it is able to cover all levels of texture, provided the skewness is lower than the Wishart case. The positive relative skewness featured by the G^0 distribution (blue curve) is found in urban areas and heterogeneous samples with a mixture of different scattering sources. Clearly, it cannot be mimiced by the $W\!K(I)$ distribution, which should still be a good model for distributed natural targets.

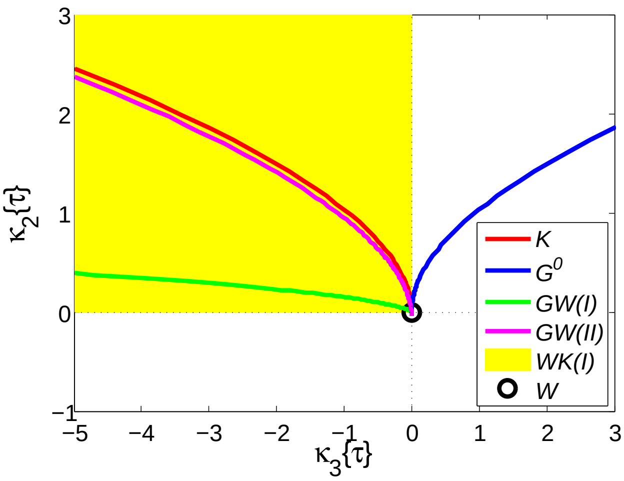

Figure 2: Texture log-cumulant diagram displaying the K, G^0, $GW(I)$, $GW(II)$ and $WK(II)$ distributions.

5 Conclusions

We have proposed the $WK(I)$ distribution as a flexible and low computational cost model for the polarimetric covariance matrix. A method for estimation of its shape parameters has also been presented. The flexibility of the distribution with respect to other models has been assessed. Rigorous derivation will be given in a future journal paper. In future work we will apply the new model to image analysis tasks, such as classification and segmentation.

References

[1] A. Lopes and F. Sery, "Optimal speckle reduction for the product model in multilook polarimetric SAR imagery and the Wishart distribution," *IEEE Trans. Geosci. Remote Sens.*, 35(3):632–647, May 1997.

[2] J.-S. Lee, M. R. Grunes, T. L. Ainsworth, D. L. Schuler, and S. R. Cloude, "Unsupervised classification using polarimetric decomposition and the complex Wishart distribution," *IEEE Trans. Geosci. Remote Sens.*, 37(5):2249–2259, Sep. 1999.

[3] K. Conradsen, A. A. Nielsen, J. Schou, and H. Skriver, "A test statistic in the complex Wishart distribution and its application to change detection in polarimetric SAR data," *IEEE Trans. Geosci. Remote Sens.*, 41(1):4–19, Jan. 2003.

[4] J.-S. Lee and E. Pottier, *Polarimetric Radar Imaging: From Basics to Applications*, ser. Optical Science and Engineering. Boca Raton, USA: CRC Press, 2009.

[5] J.-S. Lee, D. L. Schuler, R. H. Lang, and K. J. Ranson, "K-distribution for multi-look processed polarimetric SAR imagery," in *Proc. IEEE Int. Geosc. Remote Sens. Symp., IGARSS'94*, vol. 4, Pasadena, USA, Aug. 1994, pp. 2179–2181.

[6] C. C. Freitas, A. C. Frery, and A. H. Correia, "The polarimetric G distribution for SAR data analysis," *Environmetrics*, 16(1):13–31, Feb. 2005.

[7] L. Bombrun and J.-M. Beaulieu, "Fisher distribution for texture modeling of polarimetric SAR data," *IEEE Geosci. Remote Sens. Lett.*, 5(3):512–516, Jul. 2008.

[8] A. P. Doulgeris, S. N. Anfinsen, and T. Eltoft, "Classification with a non-Gaussian model for PolSAR data," *IEEE Trans. Geosci. Remote Sens.*, 46(10):2999–3009, Oct. 2008.

[9] A. C. Frery, A. H. Correia, and C. C. Freitas, "Classifying multifrequency fully polarimetric imagery with multiple sources of statistical evidence and contextual information," *IEEE Trans. Geosci. Remote Sens.*, 45(10):3098–3109, Oct. 2007.

[10] L. Bombrun, "Hierarchical segmentation of polarimetric SAR images using heterogeneous clutter models," *IEEE Trans. Geosci. Remote Sens.*, 49(2):726–737, Feb. 2011.

[11] J. A. Diaz-Garcia and R. Gutiérrez-Jáimez, "Compound and scale mixture of matricvariate and matrix variate kotz-type distributions," *J. Korean Statist. Soc.*, 39(1):75–82, Mar. 2010.

[12] S. Nadarajah, "The Kotz-type distribution with applications," *Statistics*, 37(4):341–358, Jul. 2003.

[13] S. N. Anfinsen, A. P. Doulgeris, and T. Eltoft, "Estimation of the equivalent number of looks in polarimetric synthetic aperture radar imagery," *IEEE Trans. Geosci. Remote Sens.*, 47(11):3795–3809, Nov. 2009.

[14] S. N. Anfinsen, "Statistical analysis of multilook polarimetric radar images with the Mellin transform," Ph.D. dissertation, University of Tromsø, Tromsø, Norway, May 2010.

[15] H.-C. Li, W. Hong, Y.-R. Wu, and P.-Z. Fan, "An efficient and flexible statistical model based on generalized gamma distribution for amplitude SAR images," *IEEE Trans. Geosci. Remote Sens.*, 48(6):2711–2722, Jun. 2010.

[16] P. R. Kersten and T. L. Ainsworth, "A practical amplitude distribution for SAR and POLSAR images," in *Proc. EUSAR 2010 – 8th Eur. Conf. on Synthetic Aperture Radar*, 4 pp., Aachen, Germany, 2010.

[17] J.-M. Nicolas, "Introduction aux statistique de deuxième espèce: Application des logs-moments et des logs-cumulants à l'analyse des lois d'images radar," *Traitement du Signal*, 19(3):139–167, 2002, in French, English translation in [14].

[18] S. N. Anfinsen and T. Eltoft, "Application of the matrix-variate Mellin transform to analysis of polarimetric radar images," *IEEE Trans. Geosci. Remote Sens.*, 49(6):2281–2295, Jun. 2011.

[19] K.-S. Song, "Globally convergent algorithms for estimating generalized gamma distributions in fast signal and image processing," *IEEE Trans. Image Process.*, 17(8):1233–1250, Aug. 2008.